Article citation info:
Rajab RH, Hilal YY. The integration of the fuel additives and the mathematical modeling approach to enhance the engine exhaust emissions. Combustion Engines. 0000;XXX(X):xx-xx. https://doi.org/10.19206/CE-224670

Raqeeb H. RAJAB
Yousif Yakoub HILAL

Combustion Engines
Polish Scientific Society of Combustion Engines

The integration of the fuel additives and the mathematical modeling approach to enhance the engine exhaust emissions

ARTICLE INFO

Received: 12 April 2026
Revised: 2 June 2026
Accepted: 16 June 2026
Available online: 18 August 2026

The emission characteristics of a Perkins AD4.248 four-cylinder, four-stroke diesel engine with Diesel Smoke Stop (DSS) enhancement were evaluated for several loads. The engine was operated using four parameters, including a DSS additive concentration of 3 to 6 ml×l^{-1} added to diesel fuel, a machine body vibration (MBV) of 100 to 300 ms^{-2}, an engine speed (ES) of 1500 to 2000 rpm, and an engine operation time (EOT) of 1 to 3 hours. To improve engine performance, the effects of engine optimization on engine exhaust gases, including carbon monoxide (CO), nitrogen monoxide (NO), and hydrogen sulfide (H_2S), were evaluated using Response Surface Methodology (RSM). The results showed that adding 3 ml of DSS fuel improver per liter of diesel fuel resulted in the lowest overall CO, NO, and H2S emissions. The lowest exhaust gas emissions were achieved at a DSS additive concentration of 3 ml×l^{-1}, at an engine speed of 1500 rpm, an engine operating time of 1 hour, and a vibration of 100 ms^{-2}. The RSM models demonstrated acceptable performance in predicting each exhaust emission with an accuracy of 79.13%, 79.35%, and 79.95% for CO, NO, and H_2S, respectively.

Key words: *engine speed, gas emissions, fuel improver, machine body vibration, models*

1. Introduction

The global community relies on a continuous energy supply because it is vital to many critical sectors, including manufacturing, transportation, and power generation. Fossil fuels, such as natural gas, coal, gasoline, and diesel, remain the primary sources of energy to meet today's global energy demand. However, concerns about their sustainability have led to the use of alternative fuels, which have the potential to reduce environmental pollution and decrease dependence on depleting, non-renewable fossil fuels [14].

As the global community increasingly strives to achieve net-zero emissions and sustainable development goals, fuel additives have emerged as suitable adjuncts to fossil fuels. Fuel improvers are chemical additives added to fuel to enhance combustion efficiency, improving engine performance and reducing fuel consumption. Their effect on exhaust emissions can be positive in many cases, as they reduce pollutants resulting from fuel combustion and can substantially decrease greenhouse gas emissions. Using diesel fuel improvers can help many professions transition to a more sustainable, low-carbon society while offering social and economic benefits. However, it is essential to carefully consider the impacts of diesel fuel additives on many aspects, including agricultural operations and agricultural production security, and to ensure that their effects on fuel are managed and used sustainably, while accounting for the pros and cons of these additives [3, 4]. Fuel additives mixed with conventional diesel fuels offer several benefits over pure fossil fuels, as they are non-toxic and environmentally friendly owing to their physicochemical properties [1, 4].

Alcohols can be blended as improvers with gasoline and diesel fuel. Several studies have investigated the effects of alcohol-based improvers on petrol and diesel engines. It is known that the low cetane number of alcohol fuels provides a homogeneous, lean mixture that can reduce NO_x emissions and smoke and achieve good thermal efficiency in a high-load engine [10]. However, pure alcohol has a very low cetane number and cannot be run in diesel engines. Therefore, for alcohol to operate without modification in a compression ignition (CI) engine's fuel system, it must be blended with diesel fuel. Short-chain alcohols, such as methanol and ethanol, can be blended with diesel fuel. However, longer-chain alcohols, such as butanol, are more suitable due to their higher energy content, greater stability in the mixture, and lower corrosiveness [17]. Diesel fuel additives can significantly reduce exhaust emissions by reducing pollutants from fuel combustion, particularly particulate matter. Additionally, some additives improve combustion, thereby reducing emissions of suspended particles that can harm both health and the environment. Moreover, reducing harmful pollutants and health hazards in the atmosphere, such as carbon dioxide, carbon monoxide, hydrocarbons, and NO_x emissions, and more efficient combustion can lead to lower temperatures inside the engine, which reduces the formation of nitrogen oxides and other harmful gases. However, it should be noted that the effectiveness of improvers depends on the quality of the product and its use. It is always advisable to use additives approved by the vehicle manufacturer and to follow the recommendations in the vehicle manual regarding appropriate fuel types and additives [8, 9].

Lower loads mean lower temperatures and incomplete combustion. This, together with the reduced volatility of rapeseed oil with a 20% n-hexane additive, results in inferior fuel evaporation. The higher viscosity relative to diesel fuel also adversely affects atomization. As a result, the combustion process is less efficient, and CO concentrations are higher. This effect is offset by the oxygen content in the rapeseed oil-n-hexane mixture with a 20% n-hexane addition, whereas, unlike diesel fuel, in diesel, the mixture becomes richer with increasing load and combustion temperature. A decrease in oxygen content leads to an increase in CO concentration. The NO_2 concentration is higher than that of diesel fuel due to the oxidation of NO to NO_2 caused by the oxygen content of rapeseed oil [18].

RSM is a powerful statistical method for designing experiments and optimizing the effects of process variables. It has been widely used to improve and optimize processes and products across various fields, providing a structured approach to solving critical issues. Therefore, RSM is a valuable tool in industrial and scientific research settings, helping researchers determine relationships between input and response variables by systematically varying the input variables [6, 11].

Veza et al. [38] concluded that RSM has many advantages for designing, modeling, estimating, and optimizing biofuels for internal combustion engines with satisfactory accuracy. With its predictive and optimization capabilities, the response surface methodology has the potential to help advance the optimization of biofuel-powered internal combustion engines for the transition to sustainable energy. Despite RSM's potential to predict and optimize engine performance and diesel engine exhaust emissions, comprehensive research on RSM for fuel improvers, particularly for internal combustion engines, is challenging to find. Accurately predicting exhaust gas emissions from internal combustion engines remains difficult due to the complex nature of engine operation and the various factors that influence emissions. Existing models are unable to comprehensively predict emissions across diverse operating conditions. Many current models are limited by assumptions that restrict their applicability to specific types of engines or fuels, and they often fail to account for all the dynamic interactions within an engine system [13, 41, 43]. One primary limitation in modeling exhaust emissions is the difficulty of capturing the nonlinear interactions among various engine parameters, such as air-fuel ratios, ignition timing, and post-combustion treatments. Traditional models often rely on simplified linear correlations that may not accurately reflect these intricate relationships [15].

As a review, there is a growing interest in developing models that combine empirical data and advanced statistical methods to improve prediction accuracy and adapt to varying engine conditions [25]. While significant progress has been made in modeling engine exhaust emissions, gaps persist in model accuracy and applicability across different scenarios [19]. Bridging these gaps requires more sophisticated approaches that embrace the complexity of engine dynamics and leverage advancements in data analytics and computational power [33]. Very few studies have been conducted on the combustion and emissions characteristics of an engine using Diesel Smoke Stop (DSS) fuel improver. Therefore, this study uses a DSS mixed with diesel fuel to conduct performance and emissions tests on a Perkins AD4.248 four-cylinder, four-stroke diesel engine. Furthermore, no experiments in the literature determine the optimal concentration level of the improver-diesel mixture, and no models predict exhaust gas emissions. Therefore, an RSM was used in this study to optimize and parameterize the emission parameters of a diesel engine operating on a DSS-diesel mixture.

2. Materials and methods

2.1. Experimental site and machines

The experiment was conducted in 2022, 2023, and 2024 in the open fields of Mosul University in Mosul District – Nineveh Governorate, Iraq. The site coordinates are (E43,07’59.88 – N36.23’08.26) above sea level. The experimental site was abandoned land that had not been cultivated for 8 years. The area of the experimental field was two hectares. The field's topography was flat, and the soil had a clay texture (Clay, Silt, and Sand proportions were 48.45, 26, and 25.55, respectively).

The experimental work was conducted on a four-cylinder, four-stroke engine. Table 1 shows the test engine specifications. The vibration source for the subsoiler plow is a single-armed vibrating wing plow manufactured in Turkey by UZEL Company. The wings' vibration is directly in contact with the tractor's power take-off shaft. It has the following specifications: (1) Maximum working depth of 60 cm, (2) Vibrating body width of 35.8 cm, (3) Plow weight of 260 kg, (4) PTO of 540 rpm, and (5) Required traction power of 60 hp.

Table 1. Engine specification

Parameters	Specification
Model	Perkins AD4.248 diesel
Description	4-cylinder four-stroke | liquid-cooled
Rated speed	2500 rpm
Compression ratio	16:1
Rated power	44.7 kW
Bore × stroke	101 × 127 mm
Displacement	4.1 L
Electrical system voltage	12 V
Lubrication system capacity	7.6 L
Coolant system capacity	10.4 L

2.2. Fuel test and experimental setup

The diesel fuel was prepared by blending diesel with Diesel Smoke Stop DSS at concentrations of 3–6 ml/l. Table 2 lists the properties of DSS, Table 3 lists the properties of the neat diesel and fuel diesel after blending, and Table 4 lists the experimental factors.

Table 2. Characteristics of the DSS enhancer

Parameters	Qualifications
Mixture classification	According to Regulation (EC) (CLP) 1272/2008 European Commission
Ingredients of the improver	Isoalkanes, Cyclics, Aromatics n-alkanes C10-C13, Ethylhexanoic acid, Iron salt, Ethylhexanoic acid
Hazard and toxicity of the mixture	It may be fatal if swallowed and enters the airways, and does not contain any bioaccumulative or toxic substances

The basic chemical mechanism is based on catalysis and cleaning during combustion: Catalysis: Contains organometallic compounds (e.g., barium or iron additives) which act as combustion catalysts. As the fuel burns, these metallic compounds lower the activation energy required for the oxidation of carbon molecules. This means that soot burns more rapidly and completely, even at lower temperatures, and there is less visible black smoke. Cleaning: Ashless polymeric amino detergents to dissolve and prevent carbon build-up in fuel injectors. Clean injectors produce a perfect high-precision fuel spray and do not create oxygen-deficient pockets that cause thick smoke.

Table 3. Properties of diesel fuel before and after DSS addition

Properties	Neat diesel	Diesel with DSS (3 ml×l^{-1})	Diesel with DSS (6 ml×l^{-1})
Cetane number	47	48	48
Density	0.8270	0.8250	0.8241
Flash point	76	74	73
Viscosity	2.3	2.0	1.8
Color	1.5	1.0	0.5
Sulfur content	0.863	0.854	0.835

Table 4. Factors and ranges used in the experimental design

Parameters	Values
FACR, ml×l^{-1}	3 to 6
MBV, ms^{-2}	100 to 300
ES, rpm	1500 to 2000
EOT, hr	1 to 3
Total number of tests	80

The experiments involved blending DSS and diesel to form three blends and testing their performance and emissions. They were performed at two engine speeds, ranging from 1500 to 2000 rpm, with machine body vibration between 100 and 300 ms^{-2} under the load of a subsoiler plow for 1 to 3 hours of engine operation. The results were averaged across five repeated experiments. Exhaust gas emissions were measured using a Dräger X-am 5000 three-gas analyzer that measured CO, NO, and H_2S. Technical Data of Dräger X-am 5000, operation time > 12 hr, the dimensions (W × H × D) 48 × 130 × 44 mm, weight about 250 mg, battery type of NiMH, and IP 67 degree of protection. The Dräger X-am 5000 is shown in Fig. 1.

Fig 1. Dräger X-am 5000 exhaust gas emissions measuring device

2.3. Developing RSM modeling

The study aims to build multiple models to predict CO, NO, and H_2S emissions using FACR, MBV, ES, and EOT. The factors have different levels that can be divided, as described in Table 4. The steps of developing and building multiple models are as follows:

1. RSM's first goal is to find the relationship between the independent variables and the response variable; in this study, Design-Expert Version 12 software (Stat-Ease Inc., Minneapolis, Minnesota, USA) was used to analyze the Data. Figure 2 shows a schematic diagram of the RSM model development process.

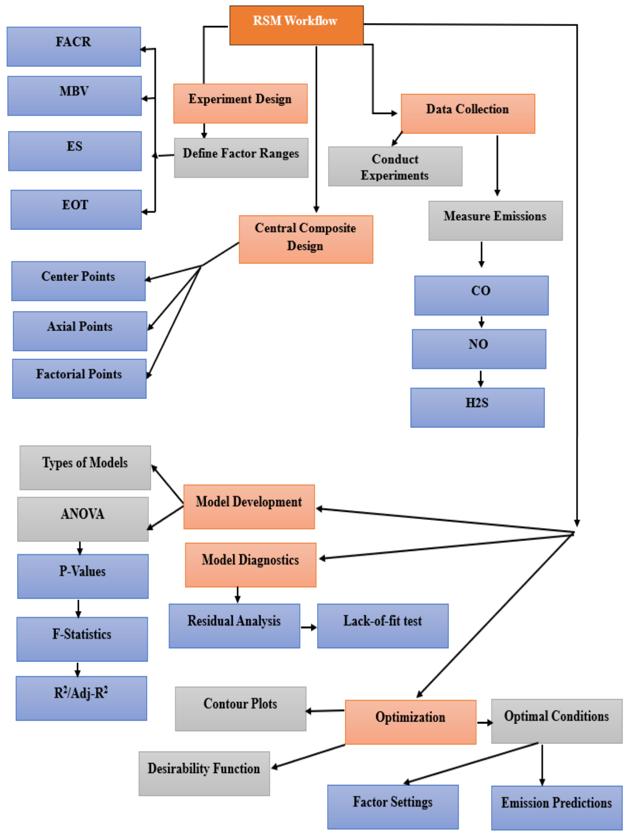

Fig. 2. Schematic diagram of the RSM model development process

2. The most appropriate polynomial mathematical models were chosen to predict the interactive effects of FACR, MBV, ES, and EOT parameters on CO, NO, and H_2S emissions.
3. Equation (1)–(6) is used to compute the R^2, the adjusted correlation coefficient (Adj. R^2), predicted correlation coefficient (Pred. R^2) and Adeq. precision.

$$R^2 = 1 - \left[\frac{SS_{residual}}{SS_{residual} + SS_{model}}\right] \tag{1}$$

$$\text{Adj. } R^2 = 1 - \left[\frac{\frac{SS_{residual}}{df_{residual}}}{\frac{SS_{residual} + SS_{model}}{df_{residual} + df_{model}}}\right] \tag{2}$$

$$\text{Pred. } R^2 = 1 - \left[\frac{PRESS}{SS_{residual} + SS_{model}}\right] \tag{3}$$

$$PRESS = \sum_{I=1}^{N} (e - 1)^2 \tag{4}$$

$$e - 1 = \frac{ei}{1 - h_{ii}} \tag{5}$$

$$\text{Adeq Precision} = \frac{(\max(\text{predicted values}) - \min(\text{predicted values}))}{\text{sqrt(average variance of the predicted values)}} \tag{6}$$

4. An analysis of variance table was used to evaluate the fitness of each developed model. The fit statistics, presented in Table 5, allowed the software to suggest the best models.

Table 5. Models proposed by the program to predict CO, NO, and H_2S emissions

	CO emission				
Source	p-value	Fit p-value	R^2 predicted	R^2 -adjusted	Model status
Linear model	< 0.0001	< 0.0001	0.5812	0.5320	
2FI model	0.0009	< 0.0001	0.7695	0.7235	Suggested
Quadratic model	0.9128	< 0.0001	0.6543	0.1311	
Cubic model	< 0.0001	< 0.0001	0.9138	–5.5535	Aliased
	NO emission				
Linear model	< 0.0001	< 0.0001	0.5872	0.5389	
2FI model	0.0004	< 0.0001	0.7834	0.7361	Suggested
Quadratic model	0.5261	< 0.0001	0.6798	0.2132	
Cubic model	< 0.0001	0.0024	0.334	0.135	Aliased
	H_2S emission				
Linear model	< 0.0001	< 0.0001	0.5489	0.5021	
2FI model	0.0028	< 0.0001	0.7857	0.7187	Suggested
Quadratic model	0.6605	< 0.0001	0.5760	0.1316	
Cubic model	< 0.0001	0.0059	0.7862	–1.5213	Aliased

Table 6. ANOVA for CO, NO, and H_2S emissions models

		CO		NO		H_2S		
Source	df	F-value	P-value	F-value	P-value	F-value	P-value	
Model	10	17.00	< 0.0001	18.06	< 0.0001	12.17	< 0.0001	Sig.
A-FACR	1	98.09	< 0.0001	111.44	< 0.0001	88.79	< 0.0001	
B-MBV	1	32.33	< 0.0001	27.76	< 0.0001	13.95	0.0004	
C-ES	1	13.52	0.0005	12.38	0.0008	4.53	0.0369	
D-EOT	1	0.0574	0.8114	0.1675	0.6836	1.77	0.1876	
AB	1	4.88	0.0305	9.50	0.0030	5.85	0.0182	
AC	1	1.49	0.2265	5.77	0.0190	0.2830	0.5965	
AD	1	1.46	0.2315	1.68	0.1999	1.59	0.2123	
BC	1	12.28	0.0008	7.06	0.0098	1.20	0.2781	
BD	1	2.76	0.1013	2.83	0.0969	3.74	0.0574	
CD	1	3.18	0.0791	1.97	0.1645	0.0186	0.8920	
Residual	69							
Lack of Fit	14	50.02	< 0.0001	24.23	< 0.0001	7.18	< 0.0001	Sig.
Pure Error	55							
Cor Total	79							

3. Results and discussion

3.1. Analysis of variance (ANOVA) for CO, NO, and H_2S emissions models

Table 6 shows the ANOVA models for the CO, NO, and H_2S emissions by FACR, MBV, and ES. The CO, NO, and H_2S models are significant, with recorded F-values of 17.00, 18.06, and 12.17, respectively. There is only a 0.01% chance that an F-value of this size caused an effect. P-values for the CO, NO, and H_2S emissions model of less than 0.0500 indicate that most terms of the model are significant. In the CO model, cases A, B, C, AB, and BC are significant model terms. The A, B, C, AB, AC, and BC are significant model terms for NO emission. While the A, B, C, and AB are significant model terms for H_2S emission. The model terms are insignificant when p-values are more than 0.1. Values greater than 0.1 indicate the model terms are not necessary. If many insignificant model terms are not counted, they are not required to support the hierarchy. In improved models, excluding these non-significant terms improves performance [22]. In the CO, NO, and H_2S models, the Lack of Fit F-values of 50.02, 24.23, and 7.18 indicate significant Lack of fit relative to the pure error, respectively. There is only a 0.01% chance that a Lack of Fit F-value this large could occur by chance.

3.2. Model of CO emissions

Accurate prediction of CO emissions is crucial for understanding their real-time dynamics and for formulating emission-reduction policies. The model determines whether the recommended model is compatible with the test results. In the CO emissions model (Table 7), the R^2 predicted of 0.7235 is in reasonable agreement with the R^2 Adjusted of 0.7695, with the difference being less than 0.2 between R^2 predicted and R^2 Adjusted. At the same time, Adeq Precision measures the signal-to-effect ratio, which should be greater than four and is desirable [20]. It achieved about 18.233 on the 2FI model (Table 7). The model in actual factor terms can be applied to predict the response for given levels of each factor. The value, in the form of adjusted and predicted values with a difference of 0.2, ensures the research follows the model and can be used to navigate the design space described. The equation in terms of actual factors can be used to predict responses for given levels of each factor, indicating that the model is highly significant and that the responses are accurate.

Table 7. 2FI model of CO emissions

Model of CO emissions	Std. Dev.	C.V. %	R^2	Adjusted R^2	Predicted R^2	Adeq Precision
	1.86	7.25	0.7913	0.7695	0.7235	18.233
$CO = 16.84852 - 0.963252FACR - 0.195023\,MBV - 0.013086\,ES + +0.012620FACR * MBV + 0.002789\,FACR * ES - 0.689815FACR * EOT + 0.000120\,MBV * ES - 0.014236\,MBV * EOT - 0.006111\,ES * EOT$						

3.3. Effect of parameters on CO emissions

The interaction effect between FACR and the MBV significantly influences the engine CO emissions, as illustrated in the response plot in Fig. 3a. The figure shows that CO emissions increase as the FACR increases. Increasing the concentration of a fuel additive may lead to increased carbon monoxide (CO) emissions due to incomplete fuel combustion. It occurs when there is insufficient oxygen in the combustion process, leading to the formation of CO rather than carbon dioxide (CO_2). Little air, incomplete combustion, and an unbalanced mixer ratio are all reasons for CO emission from the engine exhaust [21]. The widespread oxygenation and flammability properties of the Diisopropyl ether blend can reduce CO emissions [36]. In addition, Figure 3a shows that an increase in MBV due to increased load does not improve CO conversion to CO_2. The engine experiences vibrations due to overload. The fuel may not be fully combusted in the engine cylinders, leading to increased carbon monoxide formation, a gas produced by the incomplete combustion of carbon [37].

The concentration rate of the fuel additive is one of the significant influencing parameters in CO emissions. From the RSM interaction plots in Fig. 3b, the CO tends to increase as the FACR and ES increase. CO emissions in the exhaust vary with ES, but the difference is close to that with an increase in ES from 1500 to 2000 rpm. As engine speed increases, fuel consumption increases; thus, the amount of exhaust gases, including carbon monoxide, increases. Sudrajad et al. [32] found that CO exhaust emissions increase with increasing engine speed. CO is produced by burning fuel in an excess of oxygen. The ratio of carbon that cannot bind to oxygen increases fuel demand, thereby reducing thermal efficiency and increasing CO emissions. The results of Sekar et al. [27] showed that pure diesel fuel has the highest CO emissions, and a 15% blend of Diethylene Glycol and Dimethyl ether additives has the lowest.

(a) (b)

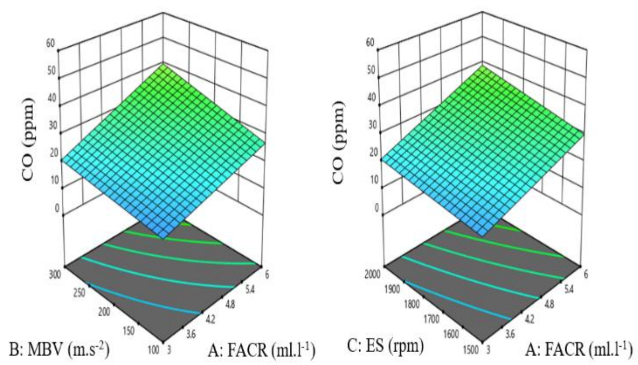

Fig. 3. Variation of CO emissions against FACR, MBV, and ES: a) the effect of interactions between MBV and FACR on CO emissions; b) the effect of interactions between ES and FACR on CO emissions

The CO emissions in the exhaust gas indicate incomplete combustion, which causes air pollution and reduces thermal efficiency. Figure 4a shows that CO emissions result from the interaction between EOT and FACR. The figure shows that CO emissions increase as EOT and FACR increase. CO emissions in the exhaust vary with EOT, but the difference is close to that with an increase in EOT from 1 to 3 hr. CO emissions are relatively low but increase by about 50% with increased engine operation time [39]. The increased CO emissions were confirmed during the test due to the greater chance of incomplete combustion. The lowest CO emissions (14 ppm) were achieved when the engine was operated at 1 hour and 3 ml×l^{-1} of FACR was added to the fuel. Measuring engine exhaust CO emissions can indicate engine performance. High CO levels indicate incomplete fuel combustion, resulting in lost power, increased fuel consumption and reduced engine efficiency [24]. Figure 4b presents a contour plot of the model's interaction between ES and MBV, showing CO emissions concentrations for different changes in ES and MBV. The figure shows that CO emissions tend to increase as ES and MBV increase in all noted speed and vibration conditions. The lowest CO emissions were achieved at an interaction between the engine's speed of 1500 rpm and a vibration rate of 100 ms^{-2}.

(a) (b)

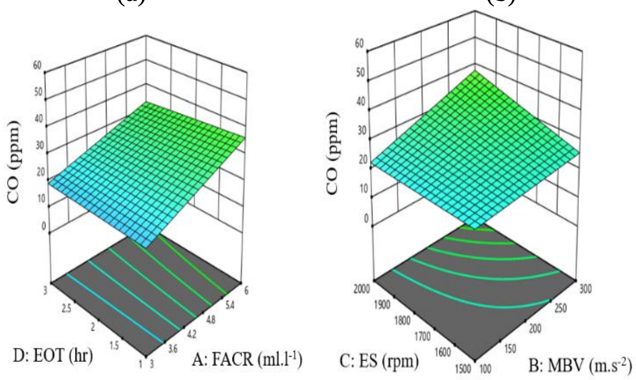

Fig.4. Variation of CO emissions against EOT, FACR, ES, and MBV: a) the effect of interactions between EOT and FACR on CO emissions; b) the effect of interactions between ES and MBV on CO emissions

Figure 5a depicts the CO emissions in the exhaust gas output from the exchanges between EOT and MBV. The curve shows CO emissions increasing as the EOT and MBV increase. The emission increase due to increased MBV is significantly greater than that due to EOT, because EOT causes a higher temperature rise that improves the conversion of CO to CO_2. Thiagarajan et al. [35] explained that CO is converted to CO_2 in the presence of oxygen and at high temperatures, where oxygen oxidizes CO. Furthermore, the rate of chemical reactions increases with increasing temperature; higher temperatures generated by complete combustion resulted in a higher conversion rate of CO to CO_2. The interaction effect between EOT and ES significantly influences the engine's CO emissions, as illustrated in the response plot in Fig. 5b. CO emissions increase as the EOT and ES increase; the increase due to increased ES is significantly greater than the increase due to EOT. The lowest CO emissions were achieved at an engine speed of 1500 rpm and an engine operating time of 1 hr.

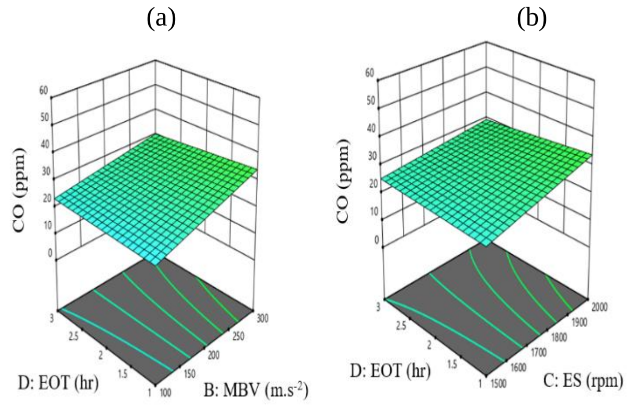

Fig. 5. Variation of CO emissions against EOT, MBV, and ES: a) the effect of interactions between EOT and MBV on CO emissions; b) the impact of interactions between EOT and ES on CO emissions

3.4. Model of NO emissions

In the NO emissions in exhaust gases model, the R^2-prediction was 0.7834, which reasonably agrees with the R^2-Adjusted of 0.7361. The difference is less than 0.2; at the same time, Adeq precision measures the signal-to-effect ratio. A ratio greater than 4 is desirable, which means the model can be used to navigate the design space. A model ratio of 9.33 indicates an adequate signal (Table 8). The model (R^2 = 0.7935) in actual-factor terms can be used to predict the response for given levels of each factor. Predicting nitrogen oxides (NOx) emissions from engine exhaust using conventional mathematical and physical methods is challenging due to the complex, variable operating conditions of engines. The accuracy of emission predictions related to the model optimization [23, 28]. Zhang et al. [42] developed a model to predict nitrous oxide emissions, and the results showed moderate predictive ability for NO_x emissions (R^2 = 0.779878). However, compared to previous models, it has better generalization and higher R^2 values. RSM is used to predict and optimize the NO_x emissions of a diesel engine under three experimental conditions. The high R-squared values, close to unity, indicate high model accuracy [9].

Table 8. 2FI model of NO emissions

Model of NO emissions	Std. Dev.	C.V. %	R²	Adjusted R²	Predicted R²	Adeq Precision
	2.08	9.33	0.7935	0.7834	0.7361	19.1802

$$NO = 32.09164 - 5.54658\,\text{FACR} - 0.150099\,\text{MBV} - 0.019945\,\text{ES} + 12.69598\,\text{EOT} + 0.015606\,\text{FACR} * \text{MBV} + 0.004867\,\text{FACR} * \text{ES} - 0.655336\,\text{FACR} * \text{EOT} + 0.000081\text{MBV} * \text{ES} - 0.012780\,\text{MBV} * \text{EOT} - 0.004268\,\text{ES} * \text{EOT}$$

3.5. Effect of parameters on NO emissions

The interaction effect between MBV and FACR significantly influences the engine's NO emissions, as illustrated in the response plot in Fig. 6a. The figure shows that NO emissions increase as the MBV and FACR increase. However, the increase in the FACR effect is greater than that due to MBV. The lowest NO emission was recorded with 3 ml×l^{-1}, due to the latent heat of the 3 ml×l^{-1} additive percentage, which is higher than that of diesel with a high additive rate. Thus, using the 3 ml×l^{-1} amount of additives decreased the peak temperature in the cylinder. Therefore, NO_x emissions are reduced with the use of a fuel additive. Elkelawy et al. [8] explained that fuel additives significantly reduce emissions in various engine types. Some engine additives can increase nitrogen oxide emissions if not used properly. Furthermore, diesel blends with appropriate additives have been shown to reduce nitrogen oxide emissions. In general, the application of fuel additives can significantly reduce harmful emissions in various engine types if used in the correct proportions. In addition, Figure 6a shows that increased MBV due to increased load will not improve NO emissions. The engine experiences vibrations due to overload. The variation in NO_x emissions with engine load across all test fuels showed that NO_x emissions increased with increasing engine load. High temperatures are the main factor in NO_x emissions. The nitrogen molecules react with oxygen, producing NO_x after the required reaction time is reached [30].

The RSM interaction plots in Fig. 6b show that NO tends to increase with increasing ES and FACR. NO emissions in the exhaust vary with ES, but the difference is close to that with an increase in ES from 1500 to 2000 rpm. As engine speed increases, the amount of NO_x emitted increases. The combustion temperature inside the engine increases with speed, leading to increased NO_x formation [34]. When the engine runs at higher speed, the number of combustion cycles per unit time increases, resulting in higher combustion temperatures and increased NO_x emissions [7].

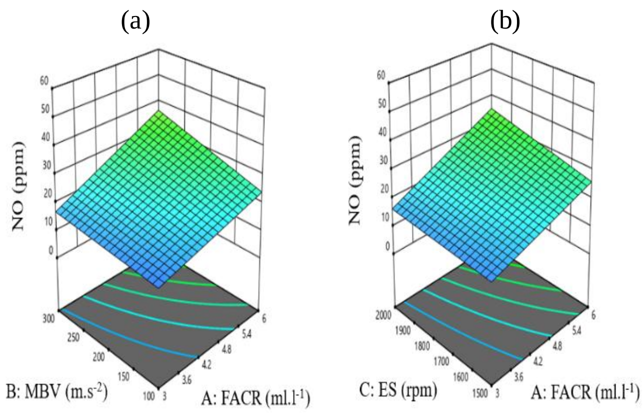

Fig. 6. Variation of NO emissions against MBV, ES, and FACR: a) the effect of interactions between MBV and FACR on NO emissions; b) the effect of interactions between ES and FACR on NO emissions

NO_x is an air pollutant that contributes to smog and acid rain and harms human health. When fuel does not burn completely, it produces undesirable compounds such as NO_x. The main reasons for incomplete combustion include insufficient oxygen in the fuel mixture, suboptimal combustion temperatures, and inefficient engine design. Practical steps to improve combustion efficiency and reduce emissions include adjusting the fuel mixture and adding fuel additives [40]. Figure 7a shows that NO emissions result from the interaction between EOT and FACR. The figure shows that NO emissions increase as EOT and FACR increase. NO emissions in the exhaust vary with EOT, but the difference is close to that with an increase in EOT from 1 to 3 hr. The lowest NO emissions (12 ppm) were achieved when the engine was operated for 1 hour, and 3 ml×l^{-1} of FACR was added to the fuel. NO_x is formed when nitrogen and oxygen in the air react at very high temperatures, conditions common in engine combustion chambers. The longer an engine runs, the greater the chance of these reactions occurring and the more NO_x will be formed [2]. NO makes up the majority of the total NO_x produced in internal combustion engines, while NO_2 makes up the remaining percentage [26].

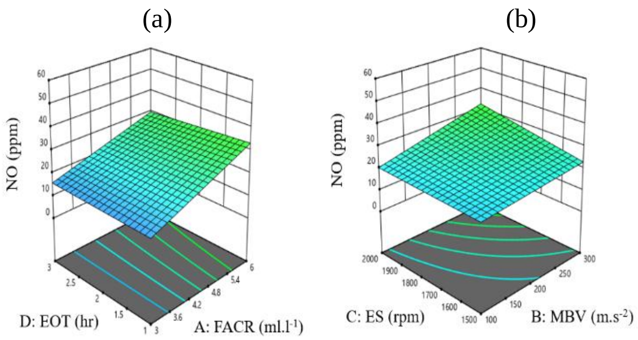

Fig. 7. Variation of NO emissions against EOT, FACR, ES, and MBV: a) the effect of interactions between EOT and FACR on NO emissions; b) the effect of interactions between ES and MBV on NO emissions

Figure 7b presents a contour plot of the model's interaction between ES and MBV, showing NO emissions concentrations for different changes in ES and MBV. The figure shows NO increase in emissions as ES and MBV increase across all noted speed and vibration conditions. The lowest NO emissions were achieved at an interaction between the engine's speed of 1500 rpm and a vibration rate of 100 ms^{-2}.

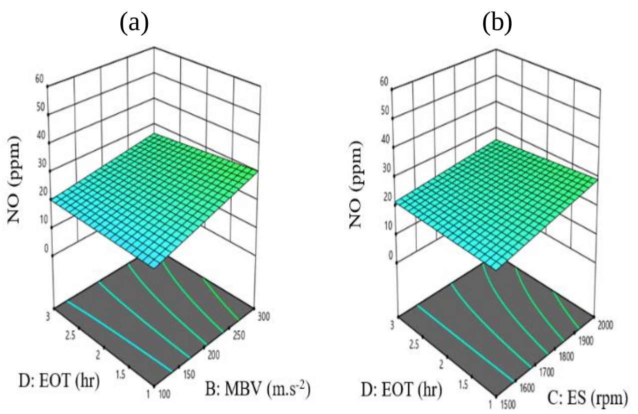

Fig. 8. Variation of NO emissions against EOT, MBV, and ES: a) the effect of interactions between EOT and MBV on NO emissions; b) the effect of interactions between EOT and ES on NO emissions

Figure 8a depicts the NO emissions in the exhaust gas output from the interactions between EOT and MBV. The response curve shows NO emissions increasing as the EOT and MBV increase. The emission increase due to increased MBV is significantly greater than that due to EOT because EOT causes a higher temperature rise, which improves NO conversion. Janulevičius et al. [16] tested the ten Massey Ferguson 6499 tractors studied. They showed that most tractors (approximately 76%) emitted nitrogen oxides during engine loads exceeding 50% of maximum torque, 21.6% between 30 and 50% of maximum torque, and only 2.3% at loads up to 30% of maximum torque. The highest nitrogen oxide emissions during actual operating cycles were recorded at speeds between 700 and 1100 rpm. The interaction effect between EOT and ES significantly influences the engine's NO emissions, as illustrated in the response plot in Fig. 8b. The figure shows that NO emissions increase with both EOT and ES; the increase due to ES is significantly greater than that due to EOT. The lowest NO emissions were achieved at an engine speed of 1500 rpm and an engine operation time of 1 hr.

3.6. Model of H_2S emissions

The accuracy of responses predicted by the software's experimental model was analyzed using variance analysis. The C.V. and R^2 values were used to determine the best-fitting model. The best-fitting model had a lower variation coefficient and a higher determination coefficient. Its significance, or lack thereof, determined the adequacy of the model. Meanwhile, the model's lack of fit must be statistically insignificant ($p > 0.05$) to fit the data well [5]. The R^2 value for the H_2S emissions model was 0.7857. The R^2-prediction reasonably agrees with the R^2-adjusted, with the difference of less than 0.2; at the same time, Adeq precision measures the signal-to-effect ratio. A ratio greater than 4 is desirable, indicating the model can effectively navigate the design space. A model ratio of 16.0715 indicates an adequate signal, as shown in Table 9.

The developed model can be used to navigate the design space in the H_2S emissions model. The predicted data in all models agreed with the experimental data, with R^2 values in these three designs close to 0.8. As stated by [29], the R^2 value should be at least 0.8 for the model to be adequate. In addition, C.V. is the standard error ratio used to predict the mean value of the actual response. In other words, C.V. could represent the model's repeatability. The model's C.V. value was 14.57. Lower values of the coefficient of variation indicated better precision and reliability of the experiment [19]. The above statistical analysis found that the 2FI model performed well in prediction. Furthermore, using the optimal model, the R^2 value for the predicted response was higher than that of most other output models. Data generated from the experimental model may have lower error than the raw data from the experiment.

Table 9. 2FI model of H_2S emissions

Model of H_2S emissions	Std. Dev.	C.V. %	R^2	Adjusted R^2	Predicted R^2	Adeq Precision
	1.02	14.57	0.7995	0.7857	0.7187	16.0715

$$\begin{aligned}H2S = {} & -3.43126 + 1.27701FACR - 0.015013\,MBV + 0.001235ES \\ & + 1.44304EOT + 0.003142FACR * MBV \\ & - 0.000276\,FACR * ES - 0.163542\,FACR * EOT \\ & + 8.52083E-06\,MBV * ES - 0.003766\,MBV \\ & * EOT - 0.000106ES * EOT\end{aligned}$$

3.7. Effect of parameters on H_2S emissions

Diesel fuel contains some sulfur. During fuel combustion, sulfur reacts with oxygen to form sulfur dioxide (SO_2). Under combustion conditions, some of the SO_2 can be converted to hydrogen sulfide (H_2S) [5]. H_2S is hazardous to human health, with concentrations of 100 ppm and above posing a risk if exposure continues for 1 to 4 hours [31]. The interaction effect between MBV and FACR significantly influences the engine's H2S emissions, as illustrated in the response plot in Fig. 9a. The figure shows that H2S emissions increase as the MBV and FACR increase. However, the increase in the FACR effect is greater than that due to MBV. The lowest H2S emission was recorded at 3 ml×l^{-1}, due to the latent heat of the 3 ml×l^{-1} additive concentration. Thus, using the 3 ml×l^{-1} amount of additives decreased the peak temperature in the cylinder. Fuel additives may include compounds that reduce the sulfur content of diesel fuel, thereby reducing hydrogen sulfide emissions. Improving the combustion process also reduces the production of harmful gases, including H_2S [38].

In addition, Fig. 9a shows that increased MBV due to increased load will not improve H_2S emissions. The engine experiences vibrations due to overload. Fayad et al. [12] showed that H_2S concentrations in the exhaust are fundamentally determined by the amount of fuel injected into the combustion chamber. As more fuel is injected in these cases, H_2S concentrations increase with increasing engine load or speed. Hydrogen reacts rapidly with sulfur, leading to high concentrations of H_2S. In the case of constant loads and variable engine speeds, H_2S decreased by 43.56% with additives added to the fuel compared to diesel. However, the H_2S concentrations did not reach hazardous levels. The RSM interaction plots in Figure 9b show that H_2S increases with increasing ES and FACR. H_2S emissions in the exhaust vary with ES, but the difference is close to that with an increase in ES from 1500 to 2000 rpm. As engine speed increases, the amount of H_2S emitted increases.

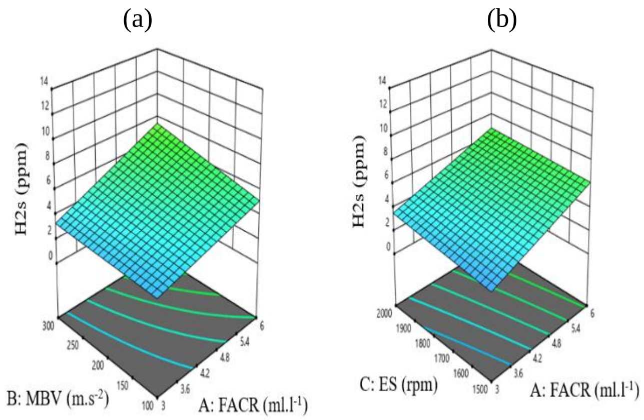

Fig. 9. Variation of H_2S emissions against FACR, MBV, and ES: a) the effect of interactions between MBV and FACR on H_2S emissions b) the effect of interactions between ES and FACR on H_2S emissions

Figure 10a shows that H_2S emissions are due to the interaction between EOT and FACR. The figure shows that H_2S emissions increase as EOT and FACR increase. H_2S emissions in the exhaust vary with EOT, but the difference is close to that with an increase in EOT from 1 to 3 hr. The increased H_2S emissions were confirmed during the test due to the greater chance of incomplete combustion. The lowest H_2S emissions were achieved when the engine was operated at 1 hour, and 3 ml×l^{-1} of FACR was added to the fuel. Measuring engine exhaust H_2S emissions can indicate engine performance. Although the H_2S emission rate was low, its accumulation could have a profound impact on the environment and human health. Figure 10b presents a contour plot of the model interaction between ES and MBV, showing H_2S emission concentrations for different changes in ES and MBV. The figure shows H_2S emissions increase as ES and MBV increase in all noted speed and vibration conditions. The lowest H_2S emissions were observed at an interaction between an engine speed of 1500 rpm and a vibration rate of 100 ms^{-2}.

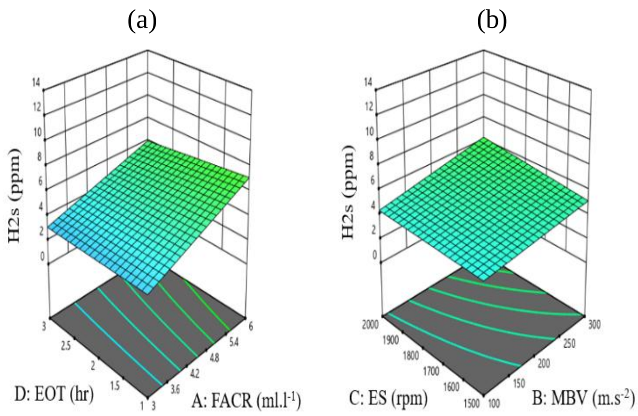

Fig. 10. Variation of H_2S emissions against EOT, FACR, ES, and MBV: a) the effect of interactions between EOT and FACR on H_2S emissions; b) the effect of interactions between ES and MBV on H_2S emissions

Figure 11a depicts the H_2S emissions in the exhaust gas output from the interactions between EOT and MBV. The response curve shows that H_2S emissions increase as EOT and MBV increase. The increase in emissions due to increased MBV is significantly greater than that due to EOT.

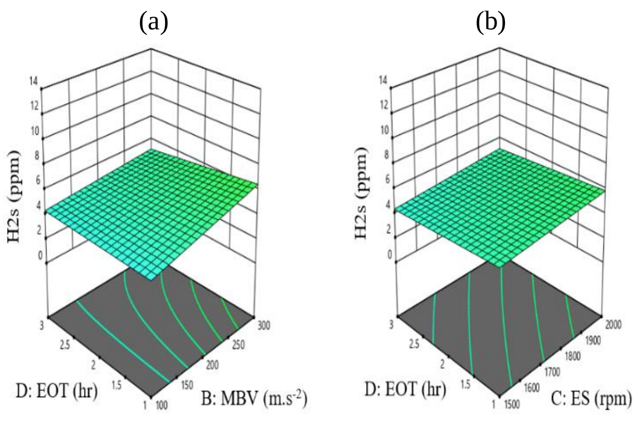

Fig. 11. Variation of H_2S emissions against EOT, MBV, and ES: a) the effect of interactions between EOT and MBV on H_2S emissions; b) the effect of interactions between EOT and ES on H_2S emissions

The interaction effect between EOT and ES significantly influences the engine's H_2S emissions, as illustrated in the response plot in Fig. 11b. The figure shows that H_2S emissions increase as EOT and ES increase; the increase due to ES is significantly greater than that due to EOT. For the engine exhausts of the fuels tested under both variable-load and variable-speed conditions, Fayad et al. [12] reported that increasing engine speed from 1250 to 3000 rpm increased H_2S emissions from 8 to 23 ppm. The results show that the H_2S concentrations in the exhaust mainly depend on the amount of fuel injected into the combustion chamber, load, and variable speed. The lowest H_2S emissions (2 ppm) were achieved at an engine speed of 1500 rpm and an engine operating time of 1 hr.

4. Conclusion

The RSM models were established to predict CO, NO, and H_2S when Diesel Smoke Stop powers an engine. The RSM results provided insights into the effects on exhaust gas and emission characteristics. Experimental data were used to develop the RSM model and study the effect of the parameters. The research results and factor impact analysis led to the following conclusions:

1. The results showed that adding a 3 ml DSS fuel improver per liter of diesel fuel recorded the lowest overall CO, NO, and H_2S emissions.
2. The DSS additive concentration of 3 $ml{\times}l^{-1}$ overlapped with an engine speed of 1500 rpm, an engine operation time of 1 hour, and a vibration of 100 $ms^{-2,}$ which recorded the lowest exhaust gas emissions.
3. CO, NO, and H_2S emissions increased as the Machine body vibration increased in all other parameters.
4. CO, NO, and H_2S emissions increased with increased engine speed and engine operation time.
5. CO, NO, and H_2S emissions increased with increasing fuel additive concentration rate (Diesel Smoke Stop), which was higher than for all other parameters.
6. It can be deduced that RSM models have many advantages in predicting and investigating emission characteristics. RSM, among other things, provides an acceptable level of performance in predicting each exhaust emission.

Intriguing research questions for future studies will focus on machine learning algorithms and computational fluid dynamics modeling to improve emissions prediction and better understand in-cylinder phenomena, along with broader practical and engineering implications for industrial and marine engine applications.

Acknowledgements

The authors sincerely thank the University of Mosul for providing the experimental facilities for conducting this study.

Nomenclature

CO	carbon monoxide
DSS	diesel Smoke Stop enhancement
EOT	engine operation time
ES	engine speed
FACR	fuel additive concentration rate
H_2S	hydrogen sulfide
MBV	machine body vibration
NO	nitrogen monoxide
RSM	response surface methodology

Bibliography

[1] Adou AI, Brelle L, Marote P, Sylvestre M, Cebriàn-Torrejòn G, Nomede-Martyr N. Physicochemical properties of coconut and waste cooking oils for biofuel production and lubrication. Fuels. 2025;6(3):57. https://doi.org/10.3390/fuels6030057

[2] Alagumalai A, Jodat A, Mahian O, Ashok B. NOx formation chemical kinetics in IC engines. NOx emission control technologies in stationary and automotive internal combustion engines. Elsevier. 2022:39-68. https://doi.org/10.1016/B978-0-12-823955-1.00002-4

[3] Awwad AA, Hilal YY, Rajab RH. The effect of diesel fuel additives on the exhaust gases of agricultural tractors during plowing. IOP Conf Ser: Earth Environ Sci. 2023;1262(9): 092001. https://doi.org/10.1088/1755-1315/1262/9/092001

[4] Ayoub HH, Rajab RH, Hilal YY. An experimental investigation on the influence of enhancers fuel and some performance indicators on a two-leg subsoiler plow. Edelweiss Appl Sci Technol. 2024;8(6):1057-1072. https://doi.org/10.55214/25768484.v8i6.2209

[5] Belo LP. Reactions, transformations and impacts of sulfur oxides during oxy-fuel combustion. Doctoral dissertation. De La Salle University. 2015. https://openresearch.newcastle.edu.au/ndownloader/files/54314294

[6] Dahlan I, Azhar EE, Hassan SR, Aziz HA, Hung YT. Statistical modeling and optimization of process parameters for 2, 4-dichlorophenoxyacetic acid removal by using AC/PDMAEMA hydrogel adsorbent: comparison of different RSM designs and ANN training methods. Water. 2022; 14(19):3061. https://doi.org/10.3390/w14193061

[7] Dev S, Lafrance S, Liko B, Guo H. A study on effect of engine operating parameters on NOx emissions and exhaust temperatures of a heavy-duty diesel engine during idling. Int J Engine Res. 2023;24(3):982-998. https://doi.org/10.1177/14680874221076087

[8] Elkelawy M, Aly Farag M, Seleem HE. Enhancing diesel engine power plant efficiency and cutting emissions with commercial fuel additives in generator systems. Pharos Eng Sci J. 2025;2(1):37-46. https://doi.org/10.21608/pesj.2025.352985.1012

[9] Elkelawy M, Bastawissi HA, Shams M. Influence of diesel engine load, waste cooking oil biodiesel blend percentage, and nanoparticles concentrations on brake thermal efficiency and NOx emissions using response surface methodology. Pharos Eng Sci J. 2025;2(1):59-74. https://doi.org/10.21608/pesj.2025.354280.1015

[10] Elkelawy M, Elkomy M, Seleem HE. Strategies for optimizing efficiency and reducing emissions footprint in spark ignition engine power plants using ethanol and CNG. Pharos Eng Sci J. 2025;2(1):107-116. https://doi.org/10.21608/pesj.2025.369010.1018

[11] Elgharbi S, Ounifi I, Boubakri A, Abdedayem A. A review of the application of response surface methodology in nanofiltration: insights into process modeling, parametric analysis, and optimization. Sep Sci Technol. 2025;60(12):1589-1603. https://doi.org/10.1080/01496395.2025.2508232

[12] Fayad MA, Chaichan MT, Dhahad HA, Al-Amiery AA, Wan Isahak WN. Reducing the effect of high sulfur content in diesel fuel on NOx emissions and PM characteristics us-

ing a PPCI mode engine and gasoline–diesel blends. ACS Omega. 2022;7(42):37328-37339. https://pubs.acs.org/doi/pdf/10.1021/acsomega.2c03878?ref=article_openPDF
[13] Hilal YY, Ishak W, Yahya A, Asha'ari ZH. Development of genetic algorithm for optimization of yield models in oil palm production. Chil J Agric Res. 2018;78(2):228-237. https://doi.org/10.4067/S0718-58392018000200228
[14] Holechek JL, Geli HM, Sawalhah MN, Valdez R. A global assessment: can renewable energy replace fossil fuels by 2050? Sustainability. 2022;14(8):4792. https://doi.org/10.3390/su14084792
[15] Klett DE, Afify EM, Srinivasan KK, Jacobs TJ. Internal combustion engines. Energy Conversion. 2017:223-255. CRC Press. https://www.taylorfrancis.com/chapters/edit/10.1201/9781315374192-11/internal-combustion-engines-david-klett-elsayed-afify-kalyan-srinivasan-timothy-jacobs
[16] Janulevičius A, Juostas A, Čiplienė A. Nitrogen-oxide emissions from diesel-engine farm tractors during real-life cycles and their correlation with the not-to-exceed operating zones. Biosyst Eng. 2017;161:93-105. https://doi.org/10.1016/j.biosystemseng.2017.06.022
[17] Li J, Wei J, Chen H, Xu Y, Liu Y, Dai Q. Study on the combustion and emission characteristics of a compression ignition engine using diesel/ethanol blend with carbon nanoadditives. Renewable Energy. 2025;246:122941. https://doi.org/10.1016/j.renene.2025.122941
[18] Longwic R, Kuszneruk M, Klepka MM. Comparative analysis of exhaust emissions from a compression-ignition engine fueled with mixtures of rapeseed oil with n-hexane and diesel fuel during selected phases of the WLTP test. Combustion Engines. 2026;205(2):39-45. https://doi.org/10.19206/CE-211740
[19] Mądziel M. Vehicle emission models and traffic simulators: a review. Energies. 2023;16(9):3941. https://doi.org/10.3390/en16093941
[20] Mahdisoozani H, Mohsenizadeh M, Bahiraei M, Kasaeian A, Daneshvar A, Goodarzi M et al. Performance enhancement of internal combustion engines through vibration control: state of the art and challenges. Appl Sci. 2019;9(3):406. https://doi.org/10.3390/app9030406
[21] Mihanović L, Jelić M, Sumić T, Radica G, Račić N. Experimental investigation of exhaust emission from marine diesel engines. 2020 5th International Conference on Smart and Sustainable Technologies (SpliTech). 2020:1-4. IEEE. https://doi.org/10.23919/SpliTech49282.2020.9243740
[22] Paw JK, Kiong TS, Kamarulzaman MK, Adam A, Hisham S, Kadirgama K et al. Advancing renewable fuel integration: A comprehensive response surface methodology approach for internal combustion engine performance and emissions optimization. Heliyon. 2023;9(11). https://doi.org/10.1016/j.heliyon.2023.e22238
[23] Qiu T, Liu Z, Lei Y, Ma X, Chen Z, Li N et al. Research on input parameter optimization for NOx deep learning prediction model. Int J Engine Res. 2024;25(12):2111-2124. https://doi.org/10.1177/14680874241272818
[24] Ramalingam K, Abdullah MZ, Elumalai PV, Reddy MV, Yafang Y, Prabhakar S et al. Production and utilization of hydrogen enriched fifth generation biofuel in LTC engines with reformed EGR. Sci Rep. 2025;15(1):25922. https://doi.org/10.1038/s41598-025-08259-w
[25] Salam S, Choudhary T, Pugazhendhi A, Verma TN, Sharma A. A review on recent progress in computational and empirical studies of compression ignition internal combustion engine. Fuel. 2020;279:118469. https://doi.org/10.1016/j.fuel.2020.118469
[26] Sciortino DD. CFD modelling of the mixture preparation in a modern gasoline direct injection engine and correlations with experimental PN emissions. Doctoral dissertation, Oxford Brookes University. 2024. https://radar.brookes.ac.uk/radar/file/74642356-ecd1-43c9-a0d4-4b7e51919653/1/Sciortino2024CFDModelling.pdf
[27] Sekar M, Selim MY, Saleh HE, Elgendi M. Utilization of hydrogen and methane as energy carriers with exhaust gas recirculation for sustainable diesel engines. Energy Convers Manag: X. 2024;23:100618. https://doi.org/10.1016/j.ecmx.2024.100618
[28] Seo J, Park S. Optimizing model parameters of artificial neural networks to predict vehicle emissions. Atmos Environ. 2023;294:119508. https://doi.org/10.1016/j.atmosenv.2022.119508
[29] Sharma P, Sarstedt M, Shmueli G, Kim KH, Thiele KO. PLS-based model selection: The role of alternative explanations in information systems research. J Assoc Inf Syst. 2019;20(4):4. https://doi.org/10.17005/1jais.00538
[30] Simsek S, Uslu S, Sahin M, Arlı F, Bilgic G. Impact of a novel fuel additive containing boron and hydrogen on diesel engine performance and emissions. Energy Sources A: Recovery Util Environ Eff. 2024;46(1):10846-10860. https://doi.org/10.1080/15567036.2021.1946621
[31] Sivakumar DB, Arulmozhi M, Sathyanarayanan S, Sridharan M. Optimization of gasoline engine operating parameters fueled with DIPE-gasoline blend: comparative evaluation between response surface methodology and fuzzy logic expert system. Process Saf Environ Prot. 2022;158: 291-307. https://doi.org/10.1016/j.psep.2021.12.015
[32] Sudrajad A, Sunardi S, Rosyadi I, Iskandar D. Evaluation of exhaust emissions of diesel engine using pyrolysis waste plastics fuel. J Mech Eng Sci Innov. 2024;4(1):75-83. https://doi.org/10.31284/j.jmesi.2024.v4i1.5971
[33] Syed S. Advanced manufacturing analytics: optimizing engine performance through real-time data and predictive maintenance. Lett High Energy Phys. 2023:184-95. https://papers.ssrn.com/sol3/Delivery.cfm?abstractid=5031293
[34] Tamilvanan A, Ashok B, Mohanraj T, Jayalakshmi P, Dhamodharan P, Sakthivel R. Effect of engine operating parameters in NOx reduction. NOx emission control technologies in stationary and automotive internal combustion engines. Elsevier. 2022:125-153. https://doi.org/10.1016/B978-0-12-823955-1.00005-X
[35] Thiagarajan S, Seetharaman S, Lokesh R, Prasanth G, Karthick B, Josephin JF et al. Impact of hydrogen-assisted combustion in a toroidal re-entrant combustion chamber powered by rapeseed oil/waste cooking oil biodiesel. Internat J Hydrogen Energy. 2025;104:367-377. https://doi.org/10.1016/j.ijhydene.2024.07.049
[36] Uppar R, Dinesha P, Kumar S. A comparative analysis of the emissions and performance of diesel fuel combustion lubricated by jatropha bio-lubricant with MWCNT additive and jojoba bio-lubricant with TiO2 additive. Discov Sustain. 2025;6(1):425. https://doi.org/10.1007/s43621-025-01265-y
[37] Verma D, Upadhyaya K. Screening the statistical impact of some independent variables on the particle size and entrapment efficiency (EE) for the design and development of curcumin-loaded PLGA-Tf nanoparticles. J Drug Deliv Ther. 2023;13(11). https://doi.org/10.22270/jddt.v13i11.6279
[38] Veza I, Spraggon M, Fattah IR, Idris M. Response surface methodology (RSM) for optimizing engine performance and emissions fueled with biofuel: Review of RSM for sustainability energy transition. Results Eng. 2023;18:101213. https://doi.org/10.1016/j.rineng.2023.101213
[39] Wang Z, Chen Y, He C, Wang D, Nie Y, Li J. Effect of improved combustion chamber design and biodiesel blend-

ing on the performance and emissions of a diesel engine. Energies. 2025;18(11):2956. https://doi.org/10.3390/en18112956

[40] Wang Y, van de Beld B, Florijn J, Holle E, Scheer R, Maes N et al. Application of fast pyrolysis bio-oil in a genset engine for combined heat and power generation. Renew Sustain Energy Rev. 2025;211:115285. https://doi.org/10.1016/j.rser.2024.115285

[41] Zbikowski M, Teodorczyk A. Machine learning for internal combustion engine optimization with hydrogen-blended fuels: a literature review. Energies. 2025;18(6):1391. https://doi.org/10.3390/en18061391

[42] Zhang Z, Liang K, Pan M, Wang H, Sang H, Zhou S et al. Exhaust emissions prediction in spark ignition engine using LightGBM optimized with the marine predators algorithm. Appl Therm Eng. 2025;275:126800. https://doi.org/10.1016/j.applthermaleng.2025.126800

[43] Zimakowska-Laskowska M, Bogdanowicz A, Kniaziewicz T. Assessment of exhaust gas concentration uniformity in a marine engine duct based on dual-point sampling and CFD modelling. Combustion Engines. 2026;205(2):3-16. https://doi.org/10.19206/CE-208912

Raqeeb H. Rajab, DEng. – Department of Petroleum and Refining Engineering, University of Mosul, Iraq.
e-mail: *raqeeb.hummadi@uomosul.edu.iq*

Yousif Yakoub Hilal, DEng. – Department of Agricultural Machines and Equipment, University of Mosul, Iraq.
e-mail: *yousif.yakoub@uomosul.edu.iq*